Application of TXRF in monitoring trace metals in particulate matter and cloud water

Khanneh Wadinga Fomba[1], Nabil Deabji[1,2], Sayf El Islam Barcha[2], Ibrahim Ouchen[2], El Mehdi Elbaramoussi[2], Rajaa Cherkaoui El Moursli[2], Mimoun Harnafi[3], Souad El Hajjaji[2], Abdelwahid Mellouki[4], and Hartmut Herrmann [1]

[1]Leibniz Institute for Tropospheric Research (TROPOS), Atmospheric Chemistry Department (ACD), Permoserstraße 15, 04318, Leipzig, Germany
[2]Faculty of Science, Mohammed V University in Rabat, 4 Avenue Ibn Battouta, B.P. 1040,10100 Rabat, Morocco
[3]Scientific Institute, Mohammed V University in Raba, Av. Ibn Batouta, B.P 703, 10106 Rabat - Morocco
[4]Institut de Combustion Aérothermique Réactivité et Environnement/OSUC-CNRS, 1C Avenue de la Recherche Scientifique, 45071 Orléans Cedex 2, France

Correspondence to: Hartmut Herrmann (herrmann@tropos.de)

Abstract. Ambient particulate matter and cloud trace metals are considered key elements of atmospheric processes as they affect air quality, environmental ecosystems and play an important role in cloud formation. However, they are often available at trace concentrations in these media such that their analysis requires high precision and sensitive techniques. In this study, different analytical methods were applied to quantify trace metals in particulate matter samples collected on quartz and polycarbonate filters as well as cloud water, using the Total reflection X-Ray Fluorescence (TXRF) technique. These methods considered the direct measurement of filter samples with and without chemical pretreatment. Direct measurements involved analysis of as collected polycarbonate and cloud water samples after they are brought onto TXRF carrier substrates. For the chemical treatment, different acid digestion procedures for PM on Quartz filters were assessed including reverse aqua regia, nitric acid and a combination of nitric acid and hydrogen peroxide solution. The effect of cold-plasma treatment of samples on polycarbonate filters prior to TXRF measurements was also investigated.

Digestion with the reverse aqua regia solution provided lower blanks and higher recovery in comparison to other tested procedures. The detection limits of the elements ranged from 0.3 to 44 ng/cm². Ca, K, Zn, and Fe showed the highest detection limits of 44, 35, 6 and 1 ng/cm² while As and Se had the lowest of 0.3 and 0.8 ng/cm², respectively. The method showed higher recovery for most trace metals when applied to commercially available reference materials and field samples. TXRF measurements showed good agreement with results obtained from ion chromatography measurements for elements such as Ca and K. Cold plasma treatment did not significantly lead to an increase in the detected concentration and the results were element-specific. Backing of the quartz filters prior to sampling showed a reduction of more than 20% of the filter blanks for elements such as V, Sr, Mn, Zn, Sb.

The methods were applied successfully on ambient particulate matter and cloud water samples collected from the Atlas Mohammed V station in Morocco and the Cape Verde Atmospheric Observatory. The obtained concentrations were within the range reported using different techniques from similar remote and background regions elsewhere, especially for elements of anthropogenic origins such as V, Pb, and Zn with concentrations of up to 10, 19 and 28 ng/m³, respectively. Enrichment factor analysis indicated that crustal matter dominated the abundance of most of the elements while anthropogenic activities also contributed to the abundance of elements such as Sb, Se, and Pb. The results confirm that TXRF is a useful complementary sensitive technique for trace metal analysis of particulate matter in the microgram range as well as in cloud water droplets.

1 Introduction

Aerosols play an important role in atmospheric processes as they control the atmospheric composition. Aerosol particles (particulate matter) provide surfaces for the adsorption of gases and atmospheric species, thereby, serving as a catalyst for heterogeneous chemical reactions. Particulate matter is the main source of condensation nuclei on which cloud droplets are formed. Clouds affect the climate, weather and are the source of precipitation and, hence, water in arid ecosystems. However, these impacts are closely related to their chemical compositions, amongst which is their elemental composition. Aerosols and cloud water trace metals play an important role in defining their physicochemical properties as they control key reactions within these media. Aerosol trace metals control atmospheric oxidation capacity and serve as a catalyst for chemical reactions that influence radical budgets and atmospheric chemical reaction rates (Losno, 1999;Herrmann et al., 2015). They provide important hints to the sources of particulate matter emission and their fate. Studies have shown that aerosol emission sources have specific profiles with certain characteristic trace metals, making elemental analysis an important tool for particulate matter source apportionment studies (VanCuren et al., 2012;Zhang et al., 2014;Miller et al., 2019), and in the quantification of PM source contributions (Harrison et al., 2012;van Pinxteren et al., 2016;Pacyna et al., 2007). Moreover, elemental analysis in cloud water provide information on cloud condensation nuclei types (Bianco et al., 2017;Ma et al., 2004), possible in-cloud heterogeneous reactions (Passananti et al., 2016;Ervens, 2015), such as the oxidation of S(IV) to sulfate (Harris et al., 2013), or trace metal influence on the HOx budget due to the Fenton reaction (Deguillaume et al., 2005). However, an assessment of their levels in mountain regions in the Saharan region where a combination of different natural and anthropogenic sources may control their abundance is lacking.

Evaluating the trace metal composition and their effects in these media requires sensitive techniques that can quantify the typically low concentration levels of metals, in these media over a wide range of particle sizes. Studies have shown that although ICP-MS (Inductively Coupled Plasma Mass Spectrometry), ICP-OES (Inductively Coupled Plasma Optical Emission Spectroscopy), AAS (Atomic Absorption Spectroscopy), are suitable sensitive techniques, most often, a larger amount of sample substance is necessary for adequate sample preparation and handling (Bennun and Sanhueza, 2010). This makes the application of alternative techniques such as the Total Reflection X-Ray Fluorescence spectrometry (TXRF) attractive in the analysis of particulate matter with very little mass, (typically in the microgram range) in comparison to the other techniques (Bulska and Ruszczyńska, 2017). The TXRF is a highly sensitive surface technique, which is a variation of the energy-dispersive X-ray fluorescence (XRF), designed such that the X-ray beam is incident at a glancing angle on a polished substrate to enable a total internal reflection of the incident beam at its surface. This setup improves on the spectral background, increases the excitation frequency of the elements, and enhances the element sensitivity compared to conventional XRF methods (Klockenkamper and von Bohlen, 2014). However, to obtain the advantages offered by the TXRF, only a very thin film of the analyte is required on a polished surface of which quartz and sapphire substrates are often used. TXRF has been shown to be applicable to soil, biological, water and sediment samples (Towett et al., 2013;Bilo et al., 2014;Stosnach, 2005). Due to its enhanced sensitivity, TXRF can easily be applied to cloud samples, as these matrices provide optimum conditions for the realization of a thin film on the carrier surface. As

with other established methods for cloud water analysis such as ICP-MS, ICP-OES as well as AAS (Xu et al.,
80 2018), sample preparation steps are few and fast.

As particulate matter is typically sampled on filter material, the application of this technique on aerosol samples
requires different sampling and sample preparation methods to obtain the requisite geometry of the sample on the
polished substrates to make use of the expected enhanced sensitivity. Recently, Prost et al. (2017) showed that by
direct sampling of aerosol particles on polished quartz substrates greased with a jelly organic paste, and subsequent
85 cold-plasma oxidation of the paste, it is possible to perform TXRF analysis directly on such substrates and obtained
measurable concentrations in the pg/m³ range. However, the limitation of this method lies in the difficulty in
controlling the thickness of the particles on the film especially in highly polluted regions where PM loading is
high, which could lead to multiple layers of particulate matter on the carrier. Studies have also shown the
applicability of TXRF on particulate matter sampled on polycarbonate filters (Wagner and Mages, 2010;Bilo et
90 al., 2018;Motellier et al., 2011) which for some cases were subsequently combusted via cold-plasma ashing and
not combusted in others, before measurement. Despite the advantage of the cold plasma ashing step in reducing
the thickness of the sample layer and attenuation of the signal, the risk of contamination, as well as variable
recovery have been reported (Woelfl et al., 2003), making its applicability for aerosol samples unclear. Different
sample preparation methods have been evaluated on PTFE membranes and polycarbonate filters, which are
95 commonly used for aerosol sampling (De La Calle et al., 2013). However, the applicability of TXRF on aerosol
particles collected on quartz fibers is not well investigated (Okuda et al., 2013). This is mainly because of the high
metal blank concentrations often obtain in this material making it less attractive to other materials such as Teflon
or polycarbonate (Upadhyay et al., 2009;Buck and Paytan, 2012). However, in comparison to other standard
techniques such as ICP-MS, ICP-AES, digestion methods of quartz filters suitable for TXRF analysis are not
100 known, especially as particles must not be fully digested in acids to obtain the required sensitivity. As many air
quality-monitoring networks sample aerosol particles on quartz filters due to the feasibility of using the same filter
sample for many analyses including elemental and organic carbon and ionic contents of the particulate matter, the
development, and applicability of analytical methods with quartz filters need further examination. This reduces
energy consumption through the deployment of fewer monitoring devices, as well as the cost of acquisition of
105 many collectors, which is a challenge for monitoring networks in developing countries

In the present study, different digestion procedures have been examined on different batches of quartz fiber filters
to assess the most preferred protocol that offers less matrix effect for quantification of trace metals using TXRF.
In addition, the role of the backing of filters on their blank concentration has been evaluated. Furthermore, the use
of plasma ashing of polycarbonate filters has been reassessed to evaluate if this procedure could be redundant for
110 samples with high particulate matter loading. The methods were applied to aerosol samples collected at the Atlas
Mohammed V (AM5) observatory and the Cape Verde Atmospheric Observatory (CVAO) during intensive field
studies lasting 2 to 3 weeks. The technique was also applied to quantify elemental concentrations in cloud water
samples from the AM5 site. The results provide the first assessment of trace metal levels at the high remote Atlas
mountain regions in northern Africa and activities that contribute to their abundance in the region.

2 Material and methods

2.1 Instrument

Trace metals were quantified using a benchtop S2-PICOFOX TXRF-spectrometer (Bruker AXS Microanalysis GmbH, Germany). The instrument is equipped with a Mo anode metal-ceramic X-Ray tube having a multilayer monochromator and an XFlash® Si drift detector, which has an area of 30 mm² with energy resolution < 160 eV for the Mn K_α-line. The Mo- K_α excitation was 17.5 keV and the instrument was operated at 750 µA and 50 kV. The typical measurement time was 500 s and the treatment of the X-ray spectra, analysis of elemental concentration and the deconvolution of spectra fluorescence peaks were performed using the SPECTRA 6.2 software.

2.2 Reagents and materials

Internal standards consisting of Gallium inductively coupled plasma (ICP) standard solution with the concentration of 1000 mg/l (Merck, Germany) and Yttrium ICP standard solution with the concentration of 1000 mg/l (Roth, Germany) mixed in the ratio 1:1 was used. High purity water deionized with Mill-Q water purification system (Millipore) was used for the dilution of standards. Hydrogen peroxide 30% (Thgeyer, Germany) solution was used for filter digestion procedures. Quartz glass discs with a 30 mm diameter and a thickness of 3 mm±0.1 mm was applied as TXRF sample carriers. They were cleaned using different cleaning solutions in three subsequent steps, involving boiling in 10% conc. HCl (Supra-Quality, ROTIPURAN, Roth Germany) and 15% conc. HNO_3 (Supra-Quality, ROTIPURAN, Roth Germany) and in a detergent solution (RBS 50, 4% concentrated). Between each solution, the carriers were rinsed with ultrapure water and treated in an ultrasonic bath for 30 mins. After cleaning, they were dried in an oven for about 3 h. Sample carriers were, thereafter, siliconized by 5 µl of a silicon solution in isopropanol (Merck, Germany) to avoid the spreading of the samples on the surface of the carriers.

2.3 Reference material

To compare the measured values with those observed with other techniques, calibrate the instrument, and validate sample preparation methods, various commercial standard reference materials were used. The NIST 2783 Standard Reference Material (SRM) air particulate matter sample and a multi-element standard solution (Lot N15521,) with a concentration of 100 mg/l for 28 elements were purchased from Sigma Aldrich, Germany and C.P.A. Ltd, Bulgaria, respectively. The NIST 2783 is an air particulate matter sample that simulates particles with an aerodynamic equivalent diameter of 2.5 µm (PM2.5) deposited on polycarbonate filter membranes.

2.4 Particulate matter and cloud water sample collection

Particulate matter and cloud water samples were collected at the AM5 observatory in Michlifen, Morocco and at the CVAO in São Vicente, Cape Verde.

The AM5 site is located in the middle of the Atlas Mountains, 2000 m a.s.l. in a predominantly hilly site (33°24'22.2"N 5°06'12.0"W) that experiences frequent changes in the wind direction. It lies in a remote region about 20 km away from the next urban cities. The aerosol particles were collected using a high-volume sampler (DIGITEL, DHA80, Switzerland) with a flow rate of 500 l/min equipped with a PM10 inlet. The collector was mounted on the roof of a container with an inlet height of about 5 meters above the ground. The aerosol particles

150 were collected on Quartz fiber filters (Munktell, MK 360) in a 12 h day-night sampling routine. The sampling routine was set to identify differences between the transport of day and night emissions to this remote site. Sampling was done for 3 weeks between August and September 2017. Cloud water was sampled using a Caltech Active Strand Cloud water Collector (CASCC2)(Demoz et al., 1996) on the roof of the container. This was done whenever the mountain was covered with clouds. The sampling time varied depending on the duration of the cloud

155 coverage and one sample was collected per cloud event. The cloud water volume ranged between 30 and 150 ml and the samples were frozen immediately after sampling.

The CVAO is located 30 m offshore the east coastline of the Sao Vicente island of the Cape Verde Island. It experiences predominantly northeast winds, providing an ideal location for monitoring long-range transport of particulate matter from Africa and Europe. At the CVAO, a five-state Berner impactor with a sampling rate of 75

160 l/min also equipped with a PM10 inlet was deployed for the collection of the aerosol particles. With the impactor system, the air is pumped through nozzles of defined diameter and particulate matter is deposited onto the impaction surface due to their inertia. The deployed Berner impactor has 5 stages with decreasing nozzle diameter stacked on top of each other enabling the collection of particles of different sizes on the impaction plates. The cut-off of the various stages (St.) was 50 - 140 nm, 140 - 420 nm, 420 - 1200 nm, 1200 - 3500 nm, 3.5 – 10 µm,

165 corresponding to St. 1 to St. 5, respectively. The collector was mounted at the top of a 30 m tall tower and particles were collected on polycarbonate membranes placed beneath the nozzles of the respective impaction plates in a 24 h sampling routine for a period of 2 weeks in January 2017. During the sampling blank filters were collected by exposing the sampler to the ambient with no air sucked through the filters. This field blank sample collection procedure was done for both the Berner impactor and the DIGITEL sample collection.

170 ## 2.5 Sample preparation

2.5.1 Bulk aerosol samples:

The quartz fiber filters from the DIGITEL were weighed before and after sampling to determine the aerosol particulate mass collected on the filters. After weighing the filters, three spots of 8 mm in diameter (ca. 2.0 cm² each) were punched out of the filters using a ceramic puncher. The punched-out filters were further cut into small

175 pieces using ceramic scissors and placed into a 10 ml acid-cleaned Teflon bomb. A total of 1.5 ml of concentrated acids of HCl and HNO_3 in the ratio 1:3 was added into the digestion bomb which was then treated in a microwave for 2 h. The digestion was done with a high-pressure digestion device with 10 ml bombs (MARS 6, CEM GmbH, Kamp-Lintfort, Germany). The main objective of digestion was to be wash-off the particles at the surface of the filters and have them in a homogenous solution which is representative of the sample that can be easily quantified.

180 This is because typical filters are too thick to be directly analyzed by TXRF. After cooling, the solution was stirred and aliquots (50 µl) of the digested solution taken and pipetted onto polished TXRF quartz carrier (3 cm diameter and 3 mm thickness). The aliquots were pipetted in series of 25 µl each on a siliconized quartz glass sample carrier to ensure confinement of the samples within a diameter of 1 cm for an effective excitation of the sample. Ga + Y was added to the solution as internal standards for the quantification of the elements. The solution was allowed to

185 evaporate on a heating plate for 10 min at 80°C. For these measurements, quartz sample carriers were used due to the high abundance of silicon on the filters. Blank samples were also analyzed with a similar procedure and the field samples were subsequently blank corrected.

The elemental concentrations of blank filters from different batches (MK 360 Lot #, 3194, 3169, 3236, 910952, 2749219) were investigated using different digestion procedure. Three digestion procedures were tested including nitric acid, reverse aqua regia ($3HNO_3:1HCL$) and $3HNO_3:1H_2O_2$ solution. They were applied to field samples to evaluate the method with a higher recovery. In addition, the effect of pre-firing of the filters on their blank values was performed.

2.5.2 Size-resolved samples

In a clean bench, the polycarbonate membranes from the five-stage cascade impactor were cut according to the number of impaction spots on the filters. For St. 1 to St. 5, filter pieces with six, three, two, one, and one, spots were cut-out, respectively. The cut-off filter pieces were placed on polished Quartz carrier substrates and spiked with 5 µl of concentrated nitric acid, to enable a planner film on the carrier surface. In addition, Ga+Y was added as an internal standard onto the sample. However, quantification was done with Ga while Y was used as a reference. The solution was allowed to evaporate on a heating plate for 10 min at 80°C and after cooling, the sample was measured. A similar procedure was performed for field blank filters. To investigate the effect of cold plasma treatment on the signal recovery, the prepared samples were measured before and after cold plasma treatment. The samples were treated in a cold plasma asher (Technics Plasma GmbH, Kirchheim Germany) operated at an oxygen pressure of 1 mbar using high purity oxygen (99.99%), at a microwave power of up to 300 W for 4 h.

2.5.3 Cloud water samples

Cloud water samples were defrosted, and 2 x 25 µl of the sample pipetted onto polished siliconized quartz carriers. The samples were further spiked with the Ga+Y internal standard solution and allowed to evaporate on a hot plate as explained above for the other samples. The dry carrier was, thereafter, transferred to the instrument for measurements. The same procedure was carried out for field blanks.

2.5.4 Standards

Similar methods were applied to the standard reference material as was used on field samples. The NIST SRM 8785 sample was prepared by microwave digestion with a similar procedure as the bulk aerosol samples. The NIST 2783 SRM was prepared using the direct measurement procedure by punching-out 0.5 cm² area of the filter and placing it on a quartz carrier and subsequent spiking with an internal standard, similar to the procedure used for the size-resolved samples. The multi-element standards were directly pipetted onto the carriers and allowed to evaporate as was done with the cloud water samples. The recoveries of the elements from the sample preparation methods were evaluated by comparing the obtained values with the reference certified values.

2.6 Measurements

All samples were measured thrice using a measurement time of 500 s, after which, it was rotated at an angle of 90° and re-measured. The measurements at the different angles were to ensure that in the cases where the sample diameter is bigger than the recommended 10 mm, the rotation will enable the sample out of the center to be measured and as such improve the probability of analyzing the entire sample effectively. The maximum values of

the measurements were then used for further analysis. Typically, for samples whose diameter are < 10 mm, there is a high reproducibility of the measurements and a coefficient of variability of less than 5% within a 95% confidence interval. However, for samples with larger areas on the carriers the variation can attain 20%. In total, 18 elements were analyzed based on their abundance in the PM and cloud water field samples. Si was not considered in these measurements due to the utilization of quartz filters and sample carriers. The lower limit of detection for the given media was estimated from the reference samples according to Klockenkämper (Reinhold Klockenkämper, 2014), $LLD = 3\,C\,x\,\sqrt{2N_{back}}/N_{net}$, where C, is the concentration of element, N_{net}, net count rate, N_{back}, background count rate. The method detection limit (MDL) for the given matrices was estimated as 3. σ_{blank}, where σ_{blank} is the standard deviation of the elements in the blank filter.

3   Results and discussions

3.1   Reference material

Reference materials were measured using the S2-PICOFOX and the values obtained were compared with the certified values provided by NIST. Figure 1 shows the plot of the determined trace metal concentrations in the standards and the certified values. The determined concentrations showed good agreement with the certified values within an 8% error margin indicating that measurements with the direct filter sample preparation method without microwave digestion is a reliable method for analyzing atmospheric particulate matter collected on thin polycarbonate filter membranes.

Similar results were obtained with the LPA multi-element standard solution revealing a good agreement between the measured and the certified values. The standard was prepared by direct pipetting of the solution on the quartz carrier surface. For elements such as Al, As, Ti, Cr, Cu, Mn, and Sb the certified concentrations were slightly higher than the measured values while for elements such as Ba, Ca, Co, K, Ni, Pb, Sr, and Zn the measured values were slightly higher than the certified values. As observed in Fig. 2, despite the variation obtained between the individual runs of the measurements, the measured mean values were often within 1% of the certified values. This result further confirms the strength of TXRF in quantifying trace elements in thin membranes and liquid samples, without further sample preparation also reported for other matrices (von Bohlen and Fernández-Ruiz, 2020).

Quartz filter was used as reference material for the microwave digestion method as described above. In principle, for analysis with TXRF, complete digestion of the filters is not essential. However, the resulting particles have to be fine and less than 10µm to avoid adsorption effects and ensure reliable measurements. Hence, for particulate matter collected on thick filter substrates dissolution of the particles is necessary prior to TXRF measurements. In the absence of certified metal concentrations on quartz fiber filters, an 8 mm diameter filter area was punched out and spiked with 100 µl of the CPA multi-element standard. After allowing them to dry for 30 min at 70°C on a hot plate, they were transferred into PTFE digestion bombs and treated with reverse aqua regia solution in a microwave. The recoveries of the high-pressure digestion treatment are presented in Table 1. The recoveries ranged from 72 to 118% except for Al where the recovery was 55 %. The high recoveries were obtained for Ba, Pb, Mo and Ca while the lower recoveries were observed for As, Ti, Sb, and Se. This is most likely because signals of these elements overlapped with other elements of the standard solution leading to high uncertainties in their quantification. This was the case with Mo and S, Ca and Sb, Ti, and Ba as well as Pb and As. The low recovery of Al from the filter indicates that the digestion process could not completely extract the Al from the quartz filter.

Contrary to other studies whereby Mo could not be determined with a Mo-anode TXRF instrument (Stosnach, 2005), the result from this CPA standard illustrates that by means of the L lines, Mo can be quantified within a given uncertainty with the S2-PICOFOX instrument. The recoveries of the other elements were above 90%. This indicates that the dissolution method can provide reliable results especially if all the particles are effectively 265 dissolved or miscible in the solvent.

To compare the direct analysis method and the microwave digestion method, the SRM 2783 was prepared using both methods and measured using the S2 PICOFOX. As shown in Fig. 3, good agreement in the determined elements was observed between the samples prepared by both methods. For elements such as Ca, Fe and Al, the 270 microwave digestion method revealed a higher recovery in comparison to the direct analytical method without digestion with a difference of about 8%. The differences between the two methods were much lower for the other elements ranging from 2 to 5%. Comparatively, the microwave digestion method, in general, revealed a higher recovery than the direct measurement method for particles on polycarbonate membranes with difference varying between 2 to 8% depending on the element. It is worth noting that, the SRM 2783 is an urban particulate matter 275 reference containing a different mineralogical property to soil samples or sediments. Hence, the observed difference in some elements may vary when other particulate matter types are measured, and this should be taken note of when comparing the results of this study with other studies.

3.1.1   Filter blanks and method recovery

The blank values of both the polycarbonate membranes and the quartz fiber filters were determined and the lower 280 limit of detection of the elements on these filters evaluated. Table 2 summarizes the absolute elemental blank concentrations of the filters as well as the method detection limits. The blank concentrations of the elements observed in the filters ranged from 80 pg to 55 ng (ca. 0.1 to 111 ng/cm²) for the polycarbonate filter membranes and from 270 pg to 566 ng (ca. 0.5 to 1133 ng/cm²) for the quartz fiber filter. This value varied between the delivery batches. Despite the variation of the concentrations per delivery batch, the range of the concentrations was typically 285 less than a factor of two for most of the elements. The method detection limit for the quartz filters was higher than that observed for the polycarbonate membranes. In comparison to detection limits and blank concentrations reported from other digestion procedures using combinations of HNO_3/HF for ICP-MS measurements (Upadhyay et al., 2009), and XRF (Okuda et al., 2013;Steinhoff et al., 2000;Itoh et al., 2018) analysis, the results from this method show lower detection limits for elements such as Ca, Zn, Fe, Ti, but higher limits for Sr. For Al and Co, 290 the blank concentrations using the methods of this study were below instrument detection limit. Comparatively to digestion procedures without HF, the application of HF (especially for analysis with ICP-MS technique) leads to an increase of the blank for elements such as Ca, Ti, Fe, which are partly embedded into the filter matrix and readily dissolved by HF, yielding to higher blanks for such elements as reported elsewhere (Upadhyay et al., 2009). This observation shows the advantages of applying TXRF for samples with low elemental concentrations using 295 quartz filters especially as complete filter digestion is not required. However, for both this study and other reported studies, Ca, K and Zn showed relatively higher blanks for quartz filters in comparison to the other elements. This suggests that quartz filters can be used in situations where higher concentrations of these elements especially, Fe, K, Zn and Ca are expected.

300   The effect of the backing of filters at higher temperatures revealed a decrease in the blank values. Three batches of filters were backed at 100 °C for 24 h, digested in reverse agua regia solution and 10 µl aliquots analyzed for their blanks. As shown in Table 3, the blank values showed a decrease in concentrations for elements such as Sb, Ca, V, Sr, Mn, Zn and Ti of more than 20%. Elements such as K, Pb, Ni and Ba, showed the lowest decrease of less than 5% while Fe, Cr, As, and Cu showed no decrease while Se showed an increase. This signifies that high-temperature backing is a useful step in reducing also the background concentrations of some elements in quartz

305   fiber filters especially when used in remote regions. Despite the lower blanks due to backing, the blank values of most of the elements were on average still higher than those in the polycarbonate filters, thereby, confirming the advantages of polycarbonate filters over quartz.

Table 4 summarizes the comparison between different acid digestion procedures on filter blank concentrations and the recovery of the elements on 3 field samples from the AM5 site. Three digestion methods; A (3:1 HNO_3: H_2O_2),

310   B (HNO_3) and C(1:3, HCl: HNO_3) were applied to these filters. Averagely, lower blank concentrations were observed using method B, followed by C and A. Using method C, a higher recovery in comparison to the other methods (A and B) was observed. For most elements, the difference ranged between 5% to 60%. This difference is likely related to the efficiency of the solution to clean the filters surface effectively and get a homogeneous mixture of the particles in the solution. Similar to other studies (Zhao et al., 2015;Dehghani et al., 2018) we observe

315   that although the inverse aqua regia solution does not provide the lowest blank values for the majority of the elements as nitric acid digestion, the recovery of the elements under the digestion protocol is significantly higher. This indicates that reverse aqua regia solution is more suitable for the dissolution of quartz filters for TXRF measurements.

3.1.2   Comparison of TXRF and ion chromatography data

320   Ca and K were analyzed with both the TXRF and the IC. Particulate matter on quartz fiber filters was dissolved in high purity deionized water through sonification and subsequent shaking for 1 h and the solution filtered through a 0.45 µm syringe filter to get rid of colloidal particles that could eventually block the chromatographic columns. Aliquots of the filtrates were analyzed for the soluble Ca and K content using both techniques. Figure 4 shows the comparison between the obtained values from both instruments. Within a 95 % confidence interval, a good

325   agreement was observed between the values from these instruments with an r² > 0.86. For both elements, slightly higher concentrations were observed with the IC with an average bias of about 7 % in comparison to the TXRF. As these are different measurement techniques with differences in detection and quantification procedures, one reason for this discrepancy could lie in the quantification uncertainties relating to the separation of neighboring peaks such as Ca (K-line: 3.692 keV), and Sb (L-line: 3.604 keV) and in the evaluation of the background signals

330   of both instruments. Differences of up to 8 % were observed between IC and TXRF for Cl in nuclear fuel samples (Dhara et al. 2012). Despite such matrix specific differences, the regressions indicate satisfactory linearity between the two techniques and high compatibility of the TXRF with other techniques when quantifying particulate matter elemental composition.

3.1.3   Effect of plasma ashing

335   Table 5 summarizes the effect of cold plasma ashing of polycarbonate samples before and after treatment. For Ca, Sr, Cr, V, Ni, Pb, Mn, and Al no significant difference was observed while for Fe, K, Ti, Cu, Rb, Mo differences

of less than 5% were observed. As, Se, Ba, Zn, and Co showed differences between 7 and 13% while Sb difference was about 30%. In general, the effect of plasma treatment was not significant for most of the elements for the samples collected at the CVAO. Hence, subsequent sample preparation of polycarbonate samples of size-resolved

340 particulate matter samples was carried out without plasma treatment. This reduces analytical time and saves costs. It is, however, worth to note that although this procedure did not significantly increase trace metal concentrations for all the elements, for samples with high organic matter content this procedure can be useful to decrease background noise and improve the signal to noise ratio and analytical sensitivity. This has been shown to be effective on biological samples (Woelfl et al. 2003) or when aerosol particles are directly collected on organic

345 pastes (Prost et al. 2017).

3.2 Field samples

3.2.1 Bulk aerosol samples

Figure 5 shows a TXRF spectrum of a bulk PM10 aerosol sample indicating some elements that were identified in the sample with the PICOFOX instrument. Box plots of the identified particulate matter trace metal

350 concentrations at the AM5 station during August and early September 2017 are shown in figure 6. The axis separates the elements according to their abundance with elements of lower concentrations on the left in ng/m³ and those with higher values on the right in µg/m³. In detail, Ca, was the most abundant element with a median concentration of 2.3 µg/m³ followed by Al (1.1 µg/m³), Fe (1.0 µg/m³), and K (0.5 µg/m³). The least abundant elements were Co (1.5 ng/m³), Cu (2.4 ng/m³), Ni (3.2 ng/m³), and Pb (4.4 ng/m³). These values did not vary

355 significantly between daytime and nighttime measurements. Indeed, the variation of the trace metals between daytime and nighttime sampling was less than 5%. Elements such as Pb, V, Cr showed a slight increase during the nighttime measurements in comparison to the daytime measurements. This indicates that these elements could have had a small nighttime source due to long-range transport from the nearby cities and the changing air mass inflow to the mountains at nighttime. The elements showed in general strong variation during the investigated

360 sampling period with a wide range of concentrations observed as revealed by their broad concentration ranges indicated by the edges of the whisker. The observed concentrations of most elements were higher than those observed at other regional background regions in Southern Africa and Europe. For elements such as Ca, Al, Fe, and Zn the concentrations in this study were higher than those reported for similar background regions in Welgegung, South Africa (Venter et al., 2017) and in Puy de Dôme, France (Vlastelic et al., 2014). Venter et al.

365 (2017) observed mean concentrations of 1.1 µg/m³ Ca, 0.17 µg/m³ Al, 1.2 µg/m³ Fe, and 0.05 µg/m³ for Zn while Vlastelic et al. (2014) observed at the Puy de Dôme mountain site, mean concentrations of 115 ng/m³ Al, 62 ng/m³ Fe, and 9.4 ng/m³ Zn. For elements such as Ni, Cu, lower concentrations were observed at AM5 (4.4, 3.0 ng/m³), respectively, in comparison to Welgegung (7.9, 6.9 ng/m³) and Puy de Dôme (1.9, 5.8 ng/m³). Sb concentration in this study were higher than at Welgegung and Puy de Dôme sites but lower than those observed

370 at other urban sites (Cheng et al., 2000). This could be partly due to interference of Sb signal with the high Ca signal in the samples as well as effect of long-range transport from nearby cities. The higher values observed in this study are mainly due to the influence of Saharan dust during the sampling period. The particulate matter mass concentration during the sampling period was up to 145 µg/m³, indicating a strong influence of Saharan dust. However, the values of this study are within reported range for mineral dust dominated particulate matter (Cardoso

375 et al., 2018;Patey et al., 2015) .

Figure 7 shows the temporal variation of the elements during the investigated period. Strong concentration fluctuations were observed for Ca, Al, Fe, Cu, and Sb. The highest concentration of Ca, Fe, Al were observed on the 12.08.2017 and 13.08.2017 while the lowest concentrations were observed on 17.08.2017 and 21.08.2017. For Cu and Sb, the 12.08.2017 and 26.08.2017 were the days with the highest and lowest concentrations, respectively.

380 Air mass trajectory investigations indicated that during these days, air mass from the Saharan desert passing through urban cities arrived at the AM5 site, while on the 26.08.2017 and 21.08.2017 the air masses mainly originated from the cities with little influence of Saharan dust. These differences indicated the strong variation observed in the air mass inflow at the remote mountainous site. Elements such as Ca, Al, Ti, Fe showed a similar temporal variation of their concentrations likewise Cu, and Zn. These similarities are indicative of their similar

385 origins either relating to their emission sources or their air mass inflow characteristics.

Typically, Ca, Al, Ti, and Fe are elements with high crustal abundance, which will indicate a strong crustal matter influence at the AM5 site during the investigated period. Cu, Sb, and Zn are elements typical of traffic, industrial emissions as well as waste incineration (Zhu et al., 2019).

3.2.2 Size resolved aerosol measurements

390 Table 6 shows the size-resolved elemental concentrations of aerosol particles observed at the CVAO during 2 weeks of measurements in January 2017. The concentration of each size fraction including the minimum, maximum, mean and standard deviation of the elements as well as their total PM10 concentrations are presented. Al was the most abundant element in the particles with a median concentration of 0.55 µg/m³ followed by Ca (0.40µg/m³), and Fe (0.36 µg/m³). Cr (0.2 ng/m³), Cu (0.33 ng/m³), Se (0.37 ng/m³), Pb (0.54 ng/m³), and As (0.96

395 ng/m³) were the least abundant elements. The difference between the least and the abundant elements was over 3 orders of magnitude indicating a strong variation in source regions and inter-daily meteorological influence on the ambient aerosol particle load at the CVAO during the investigated period.

The observed concentrations were found to be within the range of concentrations previously observed in this region, especially for PM10 elemental concentrations. Cardoso et al. (2018) observed yearly average Fe and Ca

400 concentrations of 1.8 µg/m³ and 1.4 µg/m³ in Praia, Carbo Verde while Patey et al. (2015) observed yearly mean Al concentrations of 0.76 µg/m³ at the CVAO. The differences observed between the present study and the literature values are based on the different measurement periods, yearly in comparison to the 2 weeks measurement and the different seasons of measurement, especially as seasonal trends can markedly affect particulate matter concentrations. However, for the least abundant elements, their concentration ranges were higher than those

405 reported for remote marine conditions at the CVAO. This indicates that, during the investigated period, long-range transported air masses significantly influenced the particulate matter elemental composition. In comparison to other continental measurements, the values were similar to those observed in Wien (Austria) for Ca (<231 ng/m³), Cu (< 3.7 ng/m³), Ni < (1.6 ng/m³) (Prost et al., 2017).

Generally, AM5 elemental concentrations were higher than those observed at the CVA despite the indications that

410 long-range transport of continental air masses influenced the ambient aerosol composition during the period of investigation at the CVAO. The differences observed at these stations are related to the differences in their location and hence, their different exposure to air masses of varying origins. While the CVAO is a coastal remote site, constantly influenced by oceanic and ship emissions, the AM5 is a mountainous site, influenced strongly by crustal matter resuspension from the neighboring agricultural fields and the Saharan desert. As such, the variability in the

415   elemental concentrations in these regions depends on the prevailing winds at the period of sampling as well as the local meteorological conditions. This could explain the differences in the concentrations observed at these two sites despite the influence of mineral dust in their elemental compositions.

Figure 8 shows an overview of the size distribution of given elements observed at the CVAO during the sampling period. Ca, Fe, Al, Si, Ti, Mn, Rb, Sr, were more abundant in the coarse mode particles (i.e. St. 3 to St. 5), while

420   elements such as Ni, Pb, V, Pb, Zn were more abundant in the fine mode particles (i.e. St. 1 to St. 3). These differences in the size distribution indicate their different emission sources and likely different transport patterns.

3.2.3   Method evaluation and limitations

The presented methods for extracting PM from polycarbonate and quartz fiber filters show satisfactory reproducibility on reference materials, however, for quartz fiber filters it is difficult to establish the recovery of

425   the particles on every aerosol type. Our experience shows that using the reverse aqua regia solution for digestion and washing-off of urban particulate matter from the quartz surface, a clean filter is observed with very negligible particulate matter rest on the filter. Similar observations were made also on filters that were dominated by mineral dust particulate matter mixed with soot particles. However, for field samples that have different properties from the SRM samples, the recovery of the elements via this method is difficult to estimate as the adhesion of the

430   particles to the surface may differ. We, however, recommend that for such samples, a series of tests be done to establish typical recoveries of the required elements to improve on their quantification in the given matrix. As observed in Table 2, using the digestion method, the MDL is low for most elements in the blank filters except for Ca and Zn in the polycarbonate membrane, and Ca, Zn, and K for the quartz fiber filters. Thus, if this method has to be applied to particulate matter elemental analysis, the expected concentrations should be higher for the given

435   elements. Typically, polycarbonate and Teflon filters are more suitable for trace metal analysis as they could be digested without risk of high blank values. Nevertheless, as mentioned above, the utilization of quartz fiber filters has its merits as it reduces sampling cost and monitoring cost especially if the metals of interest are within the concentration ranges that are far higher than the filter blanks. A general limitation of the PICOFOX instrument with the single Mo-anode is that heavy metals with ($Z > 43$) can only be determined through their L-lines, which

440   leads to overlapping of their signals with the K-lines of the lighter elements. This leads to higher uncertainties in the quantification of such elements especially when the element overlaps with other main matrix elements with high concentrations and broad peaks such as Cl, Ca, K, Ti, and S, in mineral dust samples. This is the case for elements such as Ru, Sb, Sn, Ba, and Mo, respectively, as observed with the recoveries of the CPA standards after filter digestion. When analyzing particulate matter samples from marine origin with high Cl and Ca concentrations,

445   care must be taken in the quantification of Ru and Sb. It is worth diluting the samples to evaluate the presence of these elements, especially as the deconvolution procedure may falsely attribute residual Cl or Ca signals to these elements due to their closeness. If the dilution does not lead to a proportionate signal, it is an indication of quantification error from the signal processing software. Despite these limitations, for investigations with limited sample material as it is the case with particulate matter samples, TXRF is quite sensitive and suitable for such

450   analysis. As shown with the elemental content of size-resolved aerosol samples with particle sizes < 140 nm, as well as those between 140 - 420 nm, the analytical errors that can be encountered using filter digestion methods for such few microgram sample mass, are typically too high in comparison to those obtained with TXRF direct

measurement method. This indeed illustrates the merit of this technique for ambient elemental particulate matter analysis.

3.2.4   Cloud water samples

The results of the determined elemental concentrations in 5 cloud water samples collected at the AM5 station during discrete cloud events are summarized in Table 7. Similar to the aerosol particle concentrations observed above, Ca (378 µg/l), and K (330 µg/l) were the most abundant elements followed by P (136 µg/l), Zn (17 µl/l), Ba (15 µg/l) and Fe (17.9 µg/l). Cr (0.25 µg/l), Rb (0.41 µg/l), Se (0.2 µg/l) and Pb (0.09 µg/l) were the least abundant elements. The median concentrations and concentration ranges of these elements are comparable to reported elemental concentrations in cloud water elsewhere. Bianco et al. (Bianco et al., 2017) reported similar concentration ranges for Zn (3.32-130 µg/l), Ti (<12.89 µg/l), Fe(<54.9 µg/l), As (<0.42 µg/l), Sb (0.02 – 0.42 µg/l), Cu (<55 µg/l) in cloud water samples collected over a contracted time period over two years at the Puy-de-Dome in France. Despite the higher number of samples that encompassed different cloud origin and formation processes in their study in comparison to the samples in this study, the similarity in the concentration range is significant. In comparison to cloud water concentrations observed in the Thuringia forest in Germany, the values of this study were generally lower, except for V whose concentration was higher (mean 1.5 µg/l, Thuringia forest 0.71 µg/l) in comparison to values observed at the Thuringia forest (Fomba et al., 2015). Despite the differences in the median and mean concentrations observed between this study and other reported results elsewhere, the reported concentrations of this study are within the range of concentrations observed in other regions in Europe. The differences in the absolute values are related to the different sample collection locations.

3.3   Crustal matter contribution to element abundance

Enrichment factor (EF) analysis was performed to evaluate the contribution of crustal matter to the trace metal levels. The EF for an element Z, is defined as (Z/Ti) aerosol/ (Z/Ti) soil. For the soil reference concentrations, the average upper continental crust values (Wedepohl, 1995) were used.

Figure 9 shows the average enrichment factors for the elements at the AM5 and the CVAO sites. From both stations, Al, Fe, Mn, Ca, K, Sr, Ba, Rb, were dominated from crustal sources. Their EF were within those of the reference upper continental crust values. Sb, As, Mo Se, showed high enrichment especially at the CVAO site in both the fine and coarse mode fraction. This indicates their non-crustal and probable anthropogenic sources. Mo and Se are emitted from oceanic emissions as well as coal combustion (Cho and Wu, 2004;Weller et al., 2008), while Sb is often used as a brake lubricant and hence often emitted from traffic activities (Pant and Harrison, 2013;He et al., 2012). These elements are also sourced from coal combustion (Pan et al., 2013;Tian et al., 2014). The other elements showed low enrichment indicating a combination of crustal and anthropogenic sources contributing to their emissions. These elements included Ni, V, Co, Cr, Cu, Zn, Pb.

Using Pearson's correlation analysis groups of elements could be identified. Fe, Mn, Ti, K, Al, showed a good correlation amongst each other with r > 0.91 within a 95% confidence interval, confirming that these elements were mostly of crustal origin. Ca, Cu, Cr, Ni, V, Pb also revealed satisfactory correlation amongst themselves although weaker in comparison to the crustal metal groups with r > 0.7) within a 90% confidence interval. This group of elements is indicative of the presence of road and urban dust, originating from resuspension of nearby roadside particles containing non-exhaust and exhaust cars emissions (Milando et al., 2016) or dust from

construction sites which are common in the nearby cities close to the AM5 sites. Pb, V, Ni are often emitted from fuel and oil combustion (Pacyna et al., 2007) while Zn, Cr, Cu are emitted from traffic activities relating to tire and brake wear, as well as metallurgical industries and waste incineration (Font et al., 2015;Harrison et al., 2012). As these sites are located in remote regions, far away from local contamination, trace metals at these sites are as a result of long-range transport from the continent over the oceans to the CVAO or from neighboring cities to the Atlas mountain.

4   Conclusion

TXRF has been investigated for its appropriateness in determining trace metal concentrations in particulate matter sampled on quartz and polycarbonate substrates as well as on cloud water samples. Methods for determining the elemental concentrations in these matrices were developed and tested on commercial standard reference material. The test results showed good agreement between determined values and commercially certified values obtained from different techniques. Extraction procedures for the preparation of particulate matter collected on membranes, quartz fiber filters using microwave digestion were assessed, and the evaluated concentrations from this method were compared with those obtained from direct measurements without sample digestion procedure. The results showed good agreement between the results obtained from both methods. It was observed that the pre-firing of quartz filters reduces the blank concentrations of some elements and that reverse aqua regia digestion provided comparatively lower blanks but higher recovery when applied to field samples. This indicated its effectiveness in cleaning aerosol particles from quartz filter surfaces. Despite its high sensitivity, care should be taken when performing aerosol multielement analysis with TXRF as overlapping of signals between K lines of light elements and L lines of heavier elements may lead to faulty conclusions. The methods were applied successfully to field samples of particulate matter and cloud water collected at different regions in Morocco and Cape Verde. The determined elemental concentrations obtained from these samples (both size-resolved and bulk particulate matter) and cloud water samples were similar to those reported elsewhere. The determined trace metals such as Fe, Ca, Al, Ti, Mn showed strong correlation amongst themselves indicating their common crustal origin. The results indicate that TXRF is a useful and complementary tool for determining elemental concentrations in the fine and coarse particulate matter as well as in cloud water.

Data availability. All data will be made available upon request by the authors.

Author Contributions. AM, HH, RCM, MH, and SH, designed the experiment at the AM5 station while, IO, EE collected the samples at the AM5 site. SIB, performed the TXRF measurements for the particles while ND, carried out the cloud water and bulk aerosol sampling at the AM5 site, performed the TXRF investigations and analysis, and assembled the data. HH and KWF designed the experiment at the CVAO. KWF compiled the analysis and prepared the manuscript. All authors reviewed and edited the manuscript and contributed to the discussion.

Competing interests. The authors declare that they have no conflict of interest.

Acknowledgment

The authors would like to thank Luis Neves for assistance in sample collection at the CVAO. This project has received funding from the European Union's Horizon 2020 research and innovation programme under grant agreement No 690958 and the German Research Foundation (DFG) project PHOSDMAP (GZ: FO1106/2-1) for 530 financial assistance. The authors would also acknowledge the support of Mrs. Julia Wilk and Cornelia Pielok for their support with the trace metal analysis.

References

535   Bennun, L., and Sanhueza, V.: A Procedure for the Improvement in the Determination of a TXRF Spectrometer
Sensitivity Curve, Anal Sci, 26, 331-335, DOI 10.2116/analsci.26.331, 2010.

Bianco, A., Vaitilingom, M., Bridoux, M., Chaumerliac, N., Pichon, J. M., Piro, J. L., and Deguillaume, L.:
Trace Metals in Cloud Water Sampled at the Puy De Dome Station, Atmosphere-Basel, 8, ARTN 225
10.3390/atmos8110225, 2017.

540   Bilo, F., Borgese, L., Cazzago, D., Zacco, A., Bontempi, E., Guarneri, R., Bernardello, M., Attuati, S., Lazo, P.,
and Depero, L. E.: TXRF analysis of soils and sediments to assess environmental contamination, Environmental
science and pollution research international, 21, 13208-13214, 10.1007/s11356-013-2203-y, 2014.

Bilo, F., Borgese, L., Wambui, A., Assi, A., Zacco, A., Federici, S., Eichert, D. M., Tsuji, K., Lucchini, R. G.,
Placidi, D., Bontempi, E., and Depero, L. E.: Comparison of multiple X-ray fluorescence techniques for

545   elemental analysis of particulate matter collected on air filters, J Aerosol Sci, 122, 1-10,
10.1016/j.jaerosci.2018.05.003, 2018.

Buck, C. S., and Paytan, A.: Evaluation of commonly used filter substrates for the measurement of aerosol trace
element solubility, Limnol Oceanogr-Meth, 10, 790-806, 10.4319/lom.2012.10.790, 2012.

Cardoso, J., Almeida, S. M., Nunes, T., Almeida-Silva, M., Cerqueira, M., Alves, C., Rocha, F., Chaves, P.,

550   Reis, M., Salvador, P., Artinano, B., and Pio, C.: Source apportionment of atmospheric aerosol in a marine dusty
environment by ionic/composition mass balance (IMB), Atmos Chem Phys, 18, 13215-13230, 10.5194/acp-18-
13215-2018, 2018.

Cheng, Z. L., Lam, K. S., Chan, L. Y., Wang, T., and Cheng, K. K.: Chemical characteristics of aerosols at
coastal station in Hong Kong. I. Seasonal variation of major ions, halogens and mineral dusts between 1995 and

555   1996, Atmos Environ, 34, 2771-2783, Doi 10.1016/S1352-2310(99)00343-X, 2000.

Cho, K., and Wu, C. Y.: Control of molybdenum emission by sorbents: Equilibrium analysis, J Environ Eng,
130, 201-204, 10.1061/(Asce)0733-9372(2004)130:2(201), 2004.

De La Calle, I., Cabaleiro, N., Romero, V., Lavilla, I., and Bendicho, C.: Sample pretreatment strategies for total
reflection X-ray fluorescence analysis: A tutorial review, Spectrochim Acta B, 90, 23-54,

560   10.1016/j.sab.2013.10.001, 2013.

Deguillaume, L., Leriche, M., Desboeufs, K., Mailhot, G., George, C., and Chaumerliac, N.: Transition metals in
atmospheric liquid phases: Sources, reactivity, and sensitive parameters, Chem Rev, 105, 3388-3431, Doi
10.1021/Cr040649c, 2005.

Dehghani, S., Moore, F., Vasiluk, L., and Hale, B. A.: The geochemical fingerprinting of geogenic particles in

565   road deposited dust from Tehran metropolis, Iran: Implications for provenance tracking, J Geochem Explor, 190,
411-423, 10.1016/j.gexplo.2018.04.011, 2018.

Demoz, B. B., Collett, J. L., and Daube, B. C.: On the Caltech Active Strand Cloudwater Collectors, Atmos Res,
41, 47-62, Doi 10.1016/0169-8095(95)00044-5, 1996.

Dhara, S., Misra, N. L., Thakur, U. K., Shah, D., Sawant, R. M., Ramakumar, K. L., and Aggarwal, S. K.: A

570   total reflection X-ray fluorescence method for the determination of chlorine at trace levels in nuclear materials
without sample dissolution, X-Ray Spectrum, 41, 316-320, 10.1002/xrs.2400, 2012.

Ervens, B.: Modeling the Processing of Aerosol and Trace Gases in Clouds and Fogs, Chem Rev, 115, 4157-
4198, 10.1021/cr5005887, 2015.

Fomba, K. W., van Pinxteren, D., Muller, K., Iinuma, Y., Lee, T., Collett, J. L., and Herrmann, H.: Trace metal
575   characterization of aerosol particles and cloud water during HCCT 2010, Atmos Chem Phys, 15, 8751-8765,
        10.5194/acp-15-8751-2015, 2015.

        Font, A., de Hoogh, K., Leal-Sanchez, M., Ashworth, D. C., Brown, R. J. C., Hansell, A. L., and Fuller, G. W.:
        Using metal ratios to detect emissions from municipal waste incinerators in ambient air pollution data, Atmos
        Environ, 113, 177-186, 10.1016/j.atmosenv.2015.05.002, 2015.

580   Harris, E., Sinha, B., van Pinxteren, D., Tilgner, A., Fomba, K. W., Schneider, J., Roth, A., Gnauk, T.,
        Fahlbusch, B., Mertes, S., Lee, T., Collett, J., Foley, S., Borrmann, S., Hoppe, P., and Herrmann, H.: Enhanced
        Role of Transition Metal Ion Catalysis During In-Cloud Oxidation of SO2, Science, 340, 727-730, DOI
        10.1126/science.1230911, 2013.

        Harrison, R. M., Jones, A. M., Gietl, J., Yin, J. X., and Green, D. C.: Estimation of the Contributions of Brake
585   Dust, Tire Wear, and Resuspension to Nonexhaust Traffic Particles Derived from Atmospheric Measurements,
        Environ Sci Technol, 46, 6523-6529, 10.1021/es300894r, 2012.

        He, M. C., Wang, X. Q., Wu, F. C., and Fu, Z. Y.: Antimony pollution in China, Sci Total Environ, 421, 41-50,
        10.1016/j.scitotenv.2011.06.009, 2012.

        Herrmann, H., Schaefer, T., Tilgner, A., Styler, S. A., Weller, C., Teich, M., and Otto, T.: Tropospheric
590   Aqueous-Phase Chemistry: Kinetics, Mechanisms, and Its Coupling to a Changing Gas Phase, Chem Rev, 115,
        4259-4334, 10.1021/cr500447k, 2015.

        Itoh, A., Yoshito Oshiro, Sotaro Azechi, Yuka Somada, Daishi Handa, Yoichi Miyagi, Kazuhiko Nakano, Akira
        Tanahara, and Arakaki, T.: Long-term Monitoring of Metal Elements in Total Suspended Particle Aerosols
        Simultaneously Collected at Three Islands in Okinawa, Japan, Asian Journal of Atmospheric Environment, 12,
595   326-337, https://doi.org/10.5572/ajae.2018.12.4.326, 2018.

        Klockenkamper, R., and von Bohlen, A.: Worldwide distribution of Total Reflection X-ray Fluorescence
        instrumentation and its different fields of application: A survey, Spectrochim Acta B, 99, 133-137,
        10.1016/j.sab.2014.06.010, 2014.

        Losno, R.: Trace metals acting as catalysts in a marine cloud: a box model study, Phys Chem Earth Pt B, 24,
600   281-286, Doi 10.1016/S1464-1909(98)00051-3, 1999.

        Ma, C. J., Tohno, S., Kasahara, M., and Hayakawa, S.: Determination of the chemical properties of residues
        retained in individual cloud droplets by XRF microprobe at SPring-8, Nucl Instrum Meth B, 217, 657-665,
        10.1016/j.nimb.2003.12.042, 2004.

        Milando, C., Huang, L., and Batterman, S.: Trends in PM2.5 emissions, concentrations and apportionments in
605   Detroit and Chicago, Atmos Environ, 129, 197-209, 10.1016/j.atmosenv.2016.01.012, 2016.

        Miller, A. J., Raduma, D. M., George, L. A., and Fry, J. L.: Source apportionment of trace elements and black
        carbon in an urban industrial area (Portland, Oregon), Atmos Pollut Res, 10, 784-794,
        10.1016/j.apr.2018.12.006, 2019.

        Motellier, S., Lhaute, K., Guiot, A., Golanski, L., Geoffroy, C., and Tardif, F.: Direct quantification of airborne
610   nanoparticles composition by TXRF after collection on filters, Journal of Physics: Conference Series, 304,
        012009, 10.1088/1742-6596/304/1/012009, 2011.

        Okuda, T., Fujimori, E., Hatoya, K., Takada, H., Kumata, H., Nakajima, F., Hatakeyama, S., Uchida, M.,
        Tanaka, S., He, K. B., Ma, Y. L., and Haraguchi, H.: Rapid and Simple Determination of Multi-Elements in

Aerosol Samples Collected on Quartz Fiber Filters by Using EDXRF Coupled with Fundamental Parameter

615   Quantification Technique, Aerosol Air Qual Res, 13, 1864-1876, 10.4209/aaqr.2012.11.0308, 2013.

Pacyna, E. G., Pacyna, J. M., Fudala, J., Strzelecka-Jastrzab, E., Hlawiczka, S., Panasiuk, D., Nitter, S., Pregger, T., Pfeiffer, H., and Friedrich, R.: Current and future emissions of selected heavy metals to the atmosphere from anthropogenic sources in Europe, Atmos Environ, 41, 8557-8566, DOI 10.1016/j.atmosenv.2007.07.040, 2007.

Pan, Y. P., Wang, Y. S., Sun, Y., Tian, S. L., and Cheng, M. T.: Size-resolved aerosol trace elements at a rural

620   mountainous site in Northern China: Importance of regional transport, Sci Total Environ, 461, 761-771, 10.1016/j.scitotenv.2013.04.065, 2013.

Pant, P., and Harrison, R. M.: Estimation of the contribution of road traffic emissions to particulate matter concentrations from field measurements: A review, Atmos Environ, 77, 78-97, 10.1016/j.atmosenv.2013.04.028, 2013.

625   Passananti, M., Vinatier, V., Delort, A. M., Mailhot, G., and Brigante, M.: Siderophores in Cloud Waters and Potential Impact on Atmospheric Chemistry: Photoreactivity of Iron Complexes under Sun-Simulated Conditions, Environ Sci Technol, 50, 9324-9332, 10.1021/acs.est.6b02338, 2016.

Patey, M. D., Achterberg, E. P., Rijkenberg, M. J., and Pearce, R.: Aerosol time-series measurements over the tropical Northeast Atlantic Ocean: Dust sources, elemental composition and mineralogy, Mar Chem, 174, 103-

630   119, 10.1016/j.marchem.2015.06.004, 2015.

Prost, J., Wobrauschek, P., and Streli, C.: Quantitative total reflection X-ray fluorescence analysis of directly collected aerosol samples, X-Ray Spectrom, 46, 454-460, 10.1002/xrs.2752, 2017.

Reinhold Klockenkämper, A. v. B.: Principles of Total Reflection XRF, in: Total-Reflection X-Ray Fluorescence Analysis and Related Methods, John Wiley & Sons, 79-125, 2014.

635   Steinhoff, G., Haupt, O., and Dannecker, W.: Fast determination of trace elements on aerosol-loaded filters by X-ray fluorescence analysis considering the inhomogeneous elemental distribution, Fresen J Anal Chem, 366, 174-177, DOI 10.1007/s002160050034, 2000.

Stosnach, H.: Environmental trace-element analysis using a benchtop total reflection X-ray, fluorescence spectrometer, Anal Sci, 21, 873-876, DOI 10.2116/analsci.21.873, 2005.

640   Tian, H. Z., Zhou, J. R., Zhu, C. Y., Zhao, D., Gao, J. J., Hao, J. M., He, M. C., Liu, K. Y., Wang, K., and Hua, S. B.: A Comprehensive Global Inventory of Atmospheric Antimony Emissions from Anthropogenic Activities, 1995-2010, Environ Sci Technol, 48, 10235-10241, 10.1021/es405817u, 2014.

Towett, E. K., Shepherd, K. D., and Cadisch, G.: Quantification of total element concentrations in soils using total X-ray fluorescence spectroscopy (TXRF), Sci Total Environ, 463, 374-388,

645   10.1016/j.scitotenv.2013.05.068, 2013.

Upadhyay, N., Majestic, B. J., Prapaipong, P., and Herckes, P.: Evaluation of polyurethane foam, polypropylene, quartz fiber, and cellulose substrates for multi-element analysis of atmospheric particulate matter by ICP-MS, Anal Bioanal Chem, 394, 255-266, 10.1007/s00216-009-2671-6, 2009.

van Pinxteren, D., Fomba, K. W., Spindler, G., Muller, K., Poulain, L., Iinuma, Y., Loschau, G., Hausmann, A.,

650   and Herrmann, H.: Regional air quality in Leipzig, Germany: detailed source apportionment of size-resolved aerosol particles and comparison with the year 2000, Faraday Discuss, 189, 291-315, 10.1039/c5fd00228a, 2016.

VanCuren, R. A., Cahill, T., Burkhart, J., Barnes, D., Zhao, Y. J., Perry, K., Cliff, S., and McConnell, J.: Aerosols and their sources at Summit Greenland - First results of continuous size- and time-resolved sampling, Atmos Environ, 52, 82-97, 10.1016/j.atmosenv.2011.10.047, 2012.

655   Venter, A. D., van Zyl, P. G., Beukes, J. P., Josipovic, M., Hendriks, J., Vakkari, V., and Laakso, L.:
     Atmospheric trace metals measured at a regional background site (Welgegund) in South Africa, Atmos Chem
     Phys, 17, 4251-4263, 10.5194/acp-17-4251-2017, 2017.

     Vlastelic, I., Suchorski, K., Sellegri, K., Colomb, A., Nauret, F., Bouvier, L., and Piro, J. L.: The trace metal
     signature of atmospheric aerosols sampled at a European regional background site (puy de Dme, France), J

660   Atmos Chem, 71, 195-212, 10.1007/s10874-014-9290-0, 2014.

     von Bohlen, A., and Fernández-Ruiz, R.: Experimental evidence of matrix effects in total-reflection X-ray
     fluorescence analysis: Coke case, Talanta, 209, 120562, https://doi.org/10.1016/j.talanta.2019.120562, 2020.

     Wagner, A., and Mages, M.: Total-Reflection X-ray fluorescence analysis of elements in size-fractionated
     particulate matter sampled on polycarbonate filters - Composition and sources of aerosol particles in Goteborg,

665   Sweden, Spectrochim Acta B, 65, 471-477, 10.1016/j.sab.2010.02.007, 2010.

     Wedepohl, K. H.: The Composition of the Continental-Crust, Geochim Cosmochim Ac, 59, 1217-1232, 1995.

     Weller, R., Woltjen, J., Piel, C., Resenberg, R., Wagenbach, D., Konig-Langlo, G., and Kriews, M.: Seasonal
     variability of crustal and marine trace elements in the aerosol at Neumayer station, Antarctica, Tellus B, 60, 742-
     752, 10.1111/j.1600-0889.2008.00372.x, 2008.

670   Woelfl, S., Mages, M., and Encina, F.: Cold plasma ashing improves the trace element detection of single
     Daphnia specimens by total reflection X-ray fluorescence spectrometry, Spectrochim Acta B, 58, 2157-2168,
     10.1016/S0584-8547(03)00196-4, 2003.

     Xu, X. M., Chen, J. M., Zhu, C., Li, J. R., Sui, X., Liu, L., and Sun, J. F.: Fog composition along the Yangtze
     River basin: Detecting emission sources of pollutants in fog water, J Environ Sci-China, 71, 2-12,

675   10.1016/j.jes.2017.09.018, 2018.

     Zhang, R., Cao, J. J., Tang, Y. R., Arimoto, R., Shen, Z. X., Wu, F., Han, Y. M., Wang, G. H., Zhang, J. Q., and
     Li, G. H.: Elemental profiles and signatures of fugitive dusts from Chinese deserts, Sci Total Environ, 472,
     1121-1129, 10.1016/j.scitotenv.2013.11.011, 2014.

     Zhao, J. H., Yan, X., Zhou, T. Y., Wang, J., Li, H. Y., Zhang, P., Ding, H., and Ding, L.: Multi-throughput

680   dynamic microwave-assisted leaching coupled with inductively coupled plasma atomic emission spectrometry
     for heavy metal analysis in soil, J Anal Atom Spectrom, 30, 1920-1926, 10.1039/c5ja00233h, 2015.

     Zhu, C., Tian, H., and Hao, J.: Global anthropogenic atmospheric emission inventory of twelve typical
     hazardous trace elements, 1995–2012, Atmos Environ, 117061, https://doi.org/10.1016/j.atmosenv.2019.117061,
     2019.

685

Table 1: Recoveries of the tested digestion procedures for quartz filters spiked with 10 µg CPA multi-element solution (n=3)

	Measured (µg)		Certified		Recovery (%)
	Mean	Std	Mean	Std.	
Al	5.47	0.94	10.00	0.28	54.7 ± 17.2
K	10.01	0.21	10.02	0.53	99.9 ± 2.1
Ca	11.16	0.24	10.00	0.29	111.6 ± 2.2
Ti	7.97	0.16	10.04	0.35	79.5 ± 2
V	9.43	0.17	10.01	0.38	94.2 ± 1.8
Cr	9.61	0.11	10.00	0.30	96.1 ± 1.1
Mn	9.71	0.16	10.00	0.28	97.1 ± 1.7
Fe	9.19	0.15	10.00	0.29	91.9 ± 1.6
Co	9.88	0.16	10.03	0.38	98.5 ± 1.6
Ni	10.57	0.14	10.00	0.41	105.7 ± 1.3
Cu	9.23	0.21	10.00	0.28	92.3 ± 2.3
Zn	9.98	0.14	10.00	0.41	99.8 ± 1.4
As	7.23	0.15	10.03	0.28	72.1 ± 2.1
Se	7.81	0.17	10.02	0.62	78 ± 2.2
Sr	13.66	1.68	10.03	0.41	136.2 ± 12.3
Mo	12.83	1.49	10.01	0.54	128.1 ± 11.6
Ag	7.44	0.76	10.01	0.29	74.3 ± 10.2
Cd	11.27	0.82	10.01	0.41	112.6 ± 7.3
Sb	8.88	0.28	9.99	0.32	88.9 ± 3.2
Ba	12.00	0.98	10.04	0.35	119.6 ± 8.2
Tl	9.65	0.16	10.00	0.28	96.5 ± 1.6
Pb	11.84	0.53	10.02	0.53	118.1 ± 4.5
Bi	10.97	0.15	9.99	0.29	109.8 ± 1.4

690

695

700

705

Table 2. The average blank filter concentrations, method detection limit (MDL) of elements in both quartz (QF) and polycarbonate (PC) filter material (Ø: 8 mm, n= 3)

QF	Conc./ng	LLD/ng	Conc[c]. $(ng/g)^{c.}$	MDL (ng/cm²) This study	a.	b.	PC	Conc./ng	LLD/ng	MDL(ng/cm²)
Ca	566.4	3.4	2,243,664	44.2	144	193	Ca	55.46	0.68	26.36
Zn	172.3	0.3	1,935	6.3	24	16.2	Zn	5.28	0.09	4.14
K	132.3	3.4	297,324	35.1	40	82.2	Fe	2.5	0.16	1.36
Fe	24.9	0.4	52,679	1.3	80	67	Ba	1.89	0.87	1.88
Sb	5.0	3.6	301	1.8	102		Cr	0.46	0.25	0.78
Cr	4.9	0.7	2,498	1.2	68	13	Sr	0.38	0.09	0.96
Ba	4.3	0.7		10.7			K	0.35	0.14	0.52
Ti	3.0	0.5	6,169	4.5	56	28.7	Ti	0.33	0.09	0.72
Cu	1.6	0.3	496	1.1	25	25.9	V	0.27	0.25	0.6
Pb	1.5	0.2	924	2.4	48	23.1	Ni	0.25	0.12	0.4
Ni	1.4	0.4	1,371	1.0	28	6.9	Pb	0.16	0.09	0.38
V	0.9	0.1	67	1.1	40	9.1	Cu	0.13	0.09	0.32
Sr	0.7	0.2	1,619	1.1			Rb	0.11	0.07	0.22
As	0.7	0.1	70	0.8	24		As	0.08	0.08	0.18
Se	0.3	0.1	25	0.3	18	39.7	Se	0.06	0.04	0.1
Mn	0.9	0.2	1,674	1.1	40	7.2				
Co	bdl		77		36					
Cd	bdl		63		47					
Al	bdl		1,196,571		432					

a. Steinhoff et al. 2000, b. Okunda et al. 2013, c. Upadhyay et al. 2009, bdl: below detection limit

710

715

720

725

730

Table 3: Effect of temperature treatment on blank concentrations showing mean values (ng), standard deviation as well as the ratio of the concentrations before and after pre-firing of filters (n=3).

Elements	Before		After		Ratio
	Mean	St.D	Mean	St.D	Before/after
Ca	148	94	108	45	1.37
Zn	13	6.1	10	4.3	1.29
K	5.7	0.8	5.4	0.8	1.05
Fe	3.5	3	3.5	1.2	1.01
Ni	1.4	1.8	1.3	0.1	1.02
Sb	1.3	1.1	0.9	0.6	1.52
Ba	0.9	0.7	0.9	0.2	1.02
Cr	0.9	0.9	0.9	0.9	1
Ti	0.3	0.1	0.2	0.1	1.21
Sr	0.2	0.1	0.1	0.1	1.36
Cu	0.13	0.05	0.13	0.09	0.98
Pb	0.07	0.01	0.06	0.01	1.04
V	0.04	0.02	0.03	0.03	1.37
As	0.04	0.01	0.04	0.01	1
Se	0.01	0	0.01	0	0.81
Mn	0.02	0.03	0.01	0	1.43

735

740

745

750

minimalhttps://doi.org/10.5194/amt-2019-428

Table 4: Elemental concentrations (ng) of different digestion procedure on blank quartz filter and field samples from the AM5 site.

Elements	Blank(n=3)						Field Samples (n=3)					
	Method A		Method B		Method C		Method A		Method B		Method C	
	Mean	St.D	Mean	St.D	Mean	St.D	Mean	St.D	Mean	St.D	Mean	St.D
Al	bdl	bdl	bdl	bdl	bdl	bdl	183	45	117	25	273	78
K	4.7	0.3	4.3	0.2	4.1	0.4	52	15	35	7	66	17
Ca	32	3.3	31	2.3	28.3	2.7	146	34	138	29	159	56
Ti	0.1	0.03	0.09	0.02	0.10	0.02	11	2.5	5.4	1.1	14.2	3.2
V	0.04	0.01	0.04	0.01	0.03	0.01	0.3	0.1	0.2	0.03	0.4	0.1
Cr	0.3	0.1	0.1	0.05	0.7	0.3	0.6	0.1	0.3	0.1	0.5	0.1
Mn	0.03	0.02	0.01	0.01	0.04	0.03	2.2	0.2	1.9	0.1	2.8	0.3
Fe	1.5	0.5	0.5	0.25	3.1	1.5	108	35	68	17	155	43
Ni	0.2	0.09	0.04	0.01	0.2	0.1	0.4	0.10	0.1	0.05	0.2	0.1
Cu	0.03	0.01	0.08	0.03	0.08	0.04	0.2	0.03	0.2	0.03	0.2	0.03
Zn	2.4	0.2	2.5	0.2	2.0	0.12	2.2	0.3	2.4	0.2	2.6	0.3
As	0.03	0.01	0.04	0.01	0.04	0.01	0.04	0.01	0.04	0.01	0.04	0.01
Se	0.01	0.01	0.01	0.01	0.01	0.01	0.01	0.01	0.01	0.01	0.01	0.01
Rb	bdl	bdl	bdl	bdl	bdl	bdl	0.2	0.1	0.1	0.1	0.3	0.1
Sr	0.06	0.01	0.05	0.01	0.05	0.01	1.2	0.1	1.0	0.1	1.4	0.3
Sb	0.5	0.2	0.3	0.2	0.6	0.3	2.8	0.4	2.4	0.1	2.5	0.3
Ba	bdl	bdl	0.08	0.02	0.04	0.01	2.0	0.3	1.8	0.1	2.3	0.3
Pb	0.09	0.02	0.80	0.20	0.04	0.01	0.5	0.1	0.5	0.1	0.6	0.2

Table 5: Effect of cold plasma treatment on samples collected on polycarbonate filters. The mean values and the
765   standard deviation from the mean are shown. Values are given in ng, (n=5).

Elements	Before		After		Ratio
	Mean	St.D	Mean	St.D	After/Before
Al	4671	475	4733	581	1.01
As	0.7	0.3	0.8	0.3	1.06
Ba	57	7.5	61	3.9	1.07
Ca	5325	250	5340	273	1.00
Co	1.01	1.6	1.14	1.3	1.13
Cr	15	0.9	15	1.5	1.00
Cu	4.7	0.1	4.9	0.6	1.04
Fe	3460	275	3544	374	1.02
K	2013	164	2058	202	1.02
Mn	65	2.5	64	2.8	0.98
Mo	25	7.9	26	14	1.04
Ni	6.6	0.5	6.6	0.5	1.00
Pb	3.6	0.4	3.6	0.7	1.00
Rb	7.7	0.2	7.9	1.1	1.03
Sb	35	28	47	5.7	1.34
Se	0.6	0.04	0.7	0.05	1.07
Sr	59	3	59	2.6	1.00
Ti	308	27	315	41	1.02
V	8.5	0.8	8.5	1	1.00
Zn	7.4	0.6	8.2	0.8	1.11

770

775
780
785
790
795
800
805
810

Table 6: Ambient size-resolved elemental concentrations (ng/m³) observed at the CVAO during the investigated period.

	St.1				St.2				St.3				St.4				St.5				PM10			
	Min	Max	Mean	St.D	Min	Max	Mean	St.D	Min	Max	Mean	St.D	Min	Max	Mean	St.D	Min	Max	Mean	St.D	Min	Max	Mean	St.D
Al	19	69	45	24	0.4	20	8.4	7.5	61	355	179	156	28	2498	711	835	19	411	182	149	49	2786	937	
K	0.4	39	10	15	0.2	8.0	2.9	3.0	1.4	69	19	24	12	935	237	306	5.8	131	64	54	39	1109	334	
Ca	0.4	103	27	41	0.0	5.0	1.6	2.1	1.5	175	36	63	20	1422	426	503	8.1	333	126	117	47	1747	607	
Ti	0.04	6.4	1.8	2.7	0.0	1.0	0.3	0.3	0.02	8.2	2.1	3.0	0.2	204	40	69	0.1	24	8.3	10	0.7	234	52	
V	0.01	0.2	0.1	0.1	0.1	1.7	0.4	0.6	0.1	1.4	0.6	0.5	0.2	15.0	3.5	5.7	0.1	1.0	0.4	0.4	0.1	17.8	3.8	
Cr	bdl	bdl	bdl		bdl	bdl	bdl		bdl	bdl	bdl		0.2	3.8	1.6	1.6	0.3	0.5	0.4	0.2	0.2	3.8	1.4	
Mn	0.02	1.5	0.5	0.7	0.1	0.2	0.2	0.1	0.02	4.3	1.0	1.6	0.1	93	17	32	0.01	10	3.2	3.9	0.3	106	22	
Fe	0.2	75	17	29	0.3	10	3.1	4.0	0.2	131	32	49	2.2	3579	649	1211	0.3	404	121	148	4.3	4070	822	
Co	0.01	0.1	0.04	0.04	0.03	0.03	0.03		0.01	0.1	0.0	0.03	0.04	1.8	0.6	0.7	0.01	0.6	0.2	0.3	0.01	2.5	0.8	
Ni	0.03	0.1	0.04	0.01	0.01	0.8	0.2	0.3	0.03	0.6	0.2	0.2	0.1	7.6	1.4	2.5	0.02	0.8	0.3	0.3	0.3	9.2	2.1	
Cu	0.01	0.04	0.02	0.01	0.02	0.03	0.02	0.01	0.01	0.1	0.04	0.03	0.03	2.0	0.5	0.6	0.01	0.2	0.1	0.1	0.1	2.3	0.6	
Zn	0.01	0.2	0.05	0.1	0.0	0.2	0.1	0.1	0.03	0.6	0.2	0.2	0.3	16	3.2	5.3	0.06	0.7	0.3	0.2	0.5	17	3.9	
As	0.01	0.6	0.3	0.4	0.0	2.7	1.7	1.5	0.03	2.5	1.6	1.4	0.1	27	11	14	0.6	10	5.3	5.2	0.01	42	13	
Se	0.01	0.01	0.01	0.01	0.02	0.1	0.03	0.02	0.02	0.2	0.1	0.1	0.1	1.8	0.5	0.6	0.01	0.1	0.1	0.0	0.1	1.9	0.6	
Rb	0.01	0.1	0.04	0.05	0.03	0.03	0.03		0.03	0.1	0.1	0.1	0.01	5.3	1.4	2.2	0.1	0.2	0.1	0.0	0.01	5.5	1.1	
Sr	0.01	1.4	0.3	0.5	0.0	0.1	0.05	0.04	0.01	2.6	0.5	0.9	0.5	30	7.6	9.9	0.2	4.5	1.8	1.5	1.0	34	10	
Mo	0.4	0.9	0.7	0.4	1.4	6.5	3.4	1.8	1.1	5.7	2.3	1.7	2.1	52	17	20	0.5	2.2	1.3	0.7	4.4	60	19	
Sb	0.2	1.8	1.0	0.8	bdl	bdl	bdl		0.9	0.9	0.9		1.4	14	6.0	5.0	0.05	5.0	2.2	1.8	0.2	19.8	7.8	
Ba	0.1	1.2	0.7	0.6	0.1	0.1	0.1	0.01	0.1	2.6	0.8	1.1	0.3	47	13	18	0.5	5.5	2.9	2.1	0.5	54	16	
Pb	0.01	0.03	0.02	0.01	0.01	0.1	0.1	0.05	0.02	0.8	0.2	0.2	0.03	13	2.7	4.8	0.04	0.3	0.2	0.1	0.1	14	3.0	

815   **Table 7:** Trace metal concentrations (µg/l) in cloud water samples collected at the AM5 station

µg/l	Min	Median	Mean	Max
Ca	0.0	359	379	682
K	144	309	331	645
Zn	bdl	9.5	17	42
Ba	8.0	12	15	25
Fe	bdl	2.4	5.1	22
Ni	1.9	4.8	6.3	13
Mn	2.2	4.4	4.4	8.9
Sr	0.1	2.0	1.9	5.8
Cu	0.8	1.7	2.5	5.6
Sb	bdl	0.0	1.0	4.8
Ti	bdl	1.1	1.5	4.6
V	bdl	0.5	0.8	2.1
Cr	bdl	0.0	0.3	0.8
Rb	0.3	0.4	0.4	0.5
Pb	bdl	0.0	0.1	0.3
Se	bdl	0.2	0.2	0.3

bdl: below detection limit

820

825

830
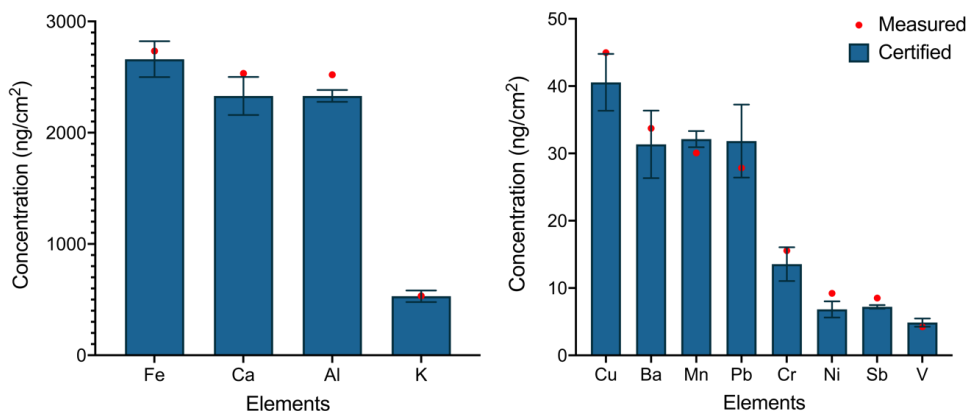
Figure 1: Plot of measured metal concentrations of NIST SRM 2783 sample using direct sample preparation method without microwave digestion.

835
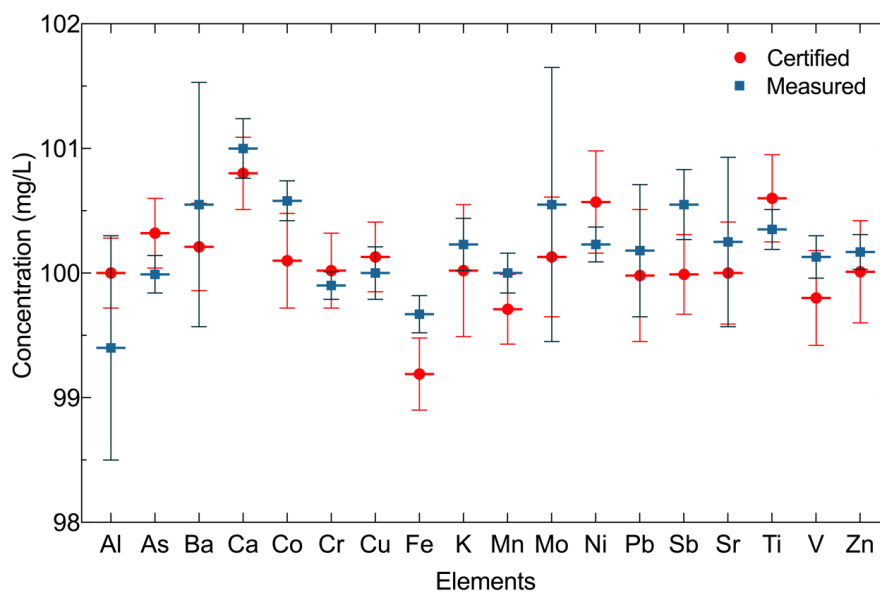
Figure 2: Good agreement observed between measured and certified values of metals in the multi-element standard solution.

840
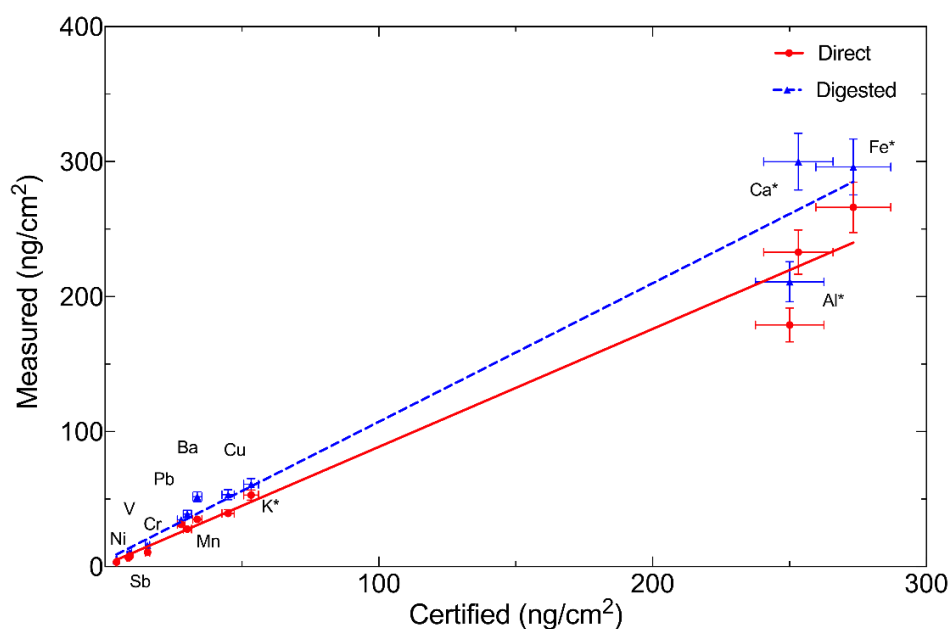
Figure 3: Comparison of microwave digestion and direct analysis method using SRM 2783 samples on polycarbonate membranes.

845
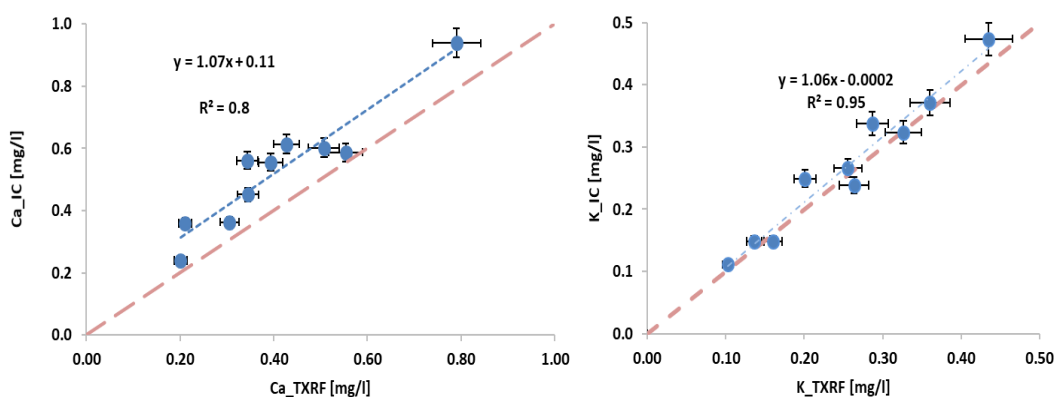
Figure 4: Comparison of Ca and K values of aerosol extracts in water measured by TXRF and ion Chromatography ICS 9000.

850
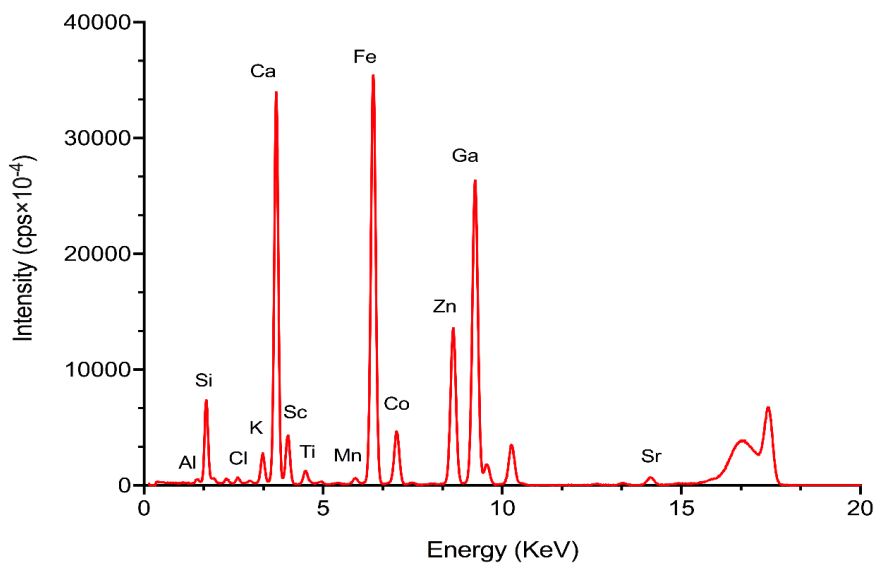
Figure 5: TXRF spectra of particulate matter samples collected at the AM5 station and measured with the Mo-excitation anode.
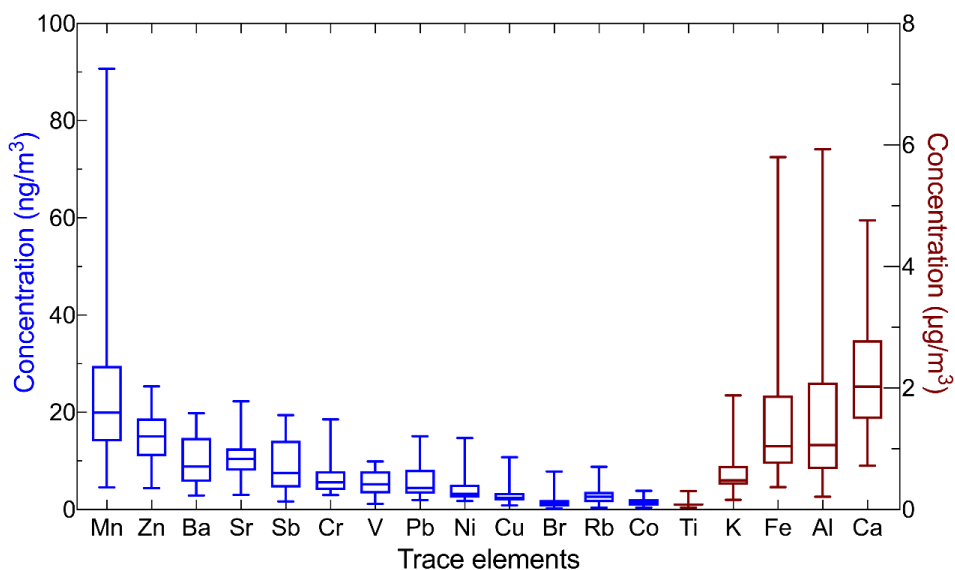
Figure 6: Box plots of ambient aerosol trace metal concentrations observed at the AM5 station during August and early September 2017
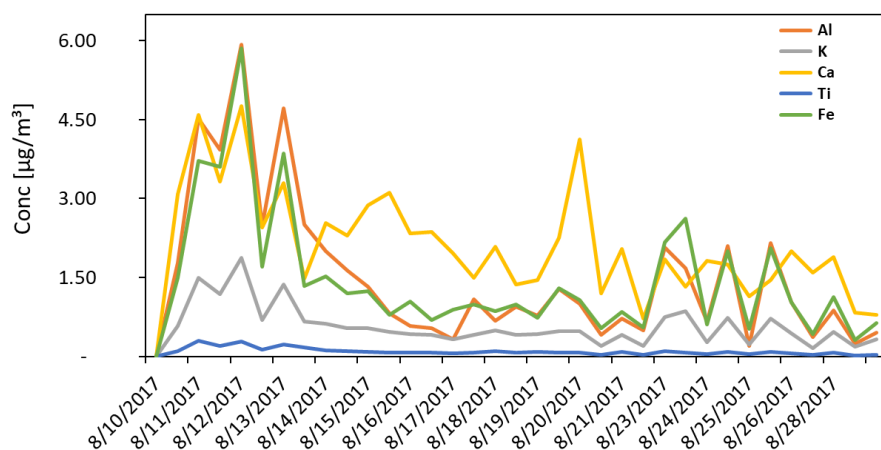
Figure 7: Temporal variation of elements observed at the AM5 during the measurement period
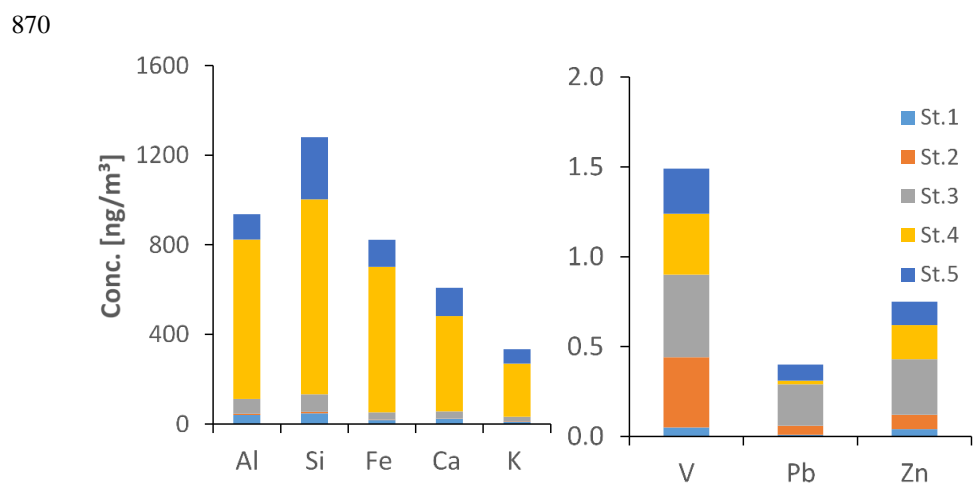
Figure 8: Size distribution of given elements with Fe, Ca, K, Al found in larger particles while V, Pb, Zn are found in smaller particles
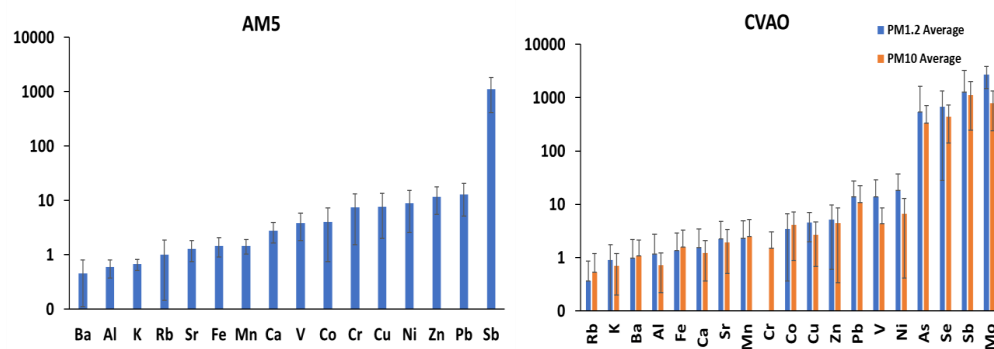
Figure 9: Crustal enrichment factors of samples collected at the AM5 and the CVAO sorted in ascending order of the enrichment of the observed elements

885

890